Since January 2020 Elsevier has created a COVID-19 resource centre with free information in English and Mandarin on the novel coronavirus COVID-19. The COVID-19 resource centre is hosted on Elsevier Connect, the company's public news and information website.

Phytomedicine 102 (2022) 154154

Contents lists available at ScienceDirect

Phytomedicine

journal homepage: www.elsevier.com/locate/phymed

Original Article

Polygoni multiflori radix extracts inhibit SARS-CoV-2 pseudovirus entry in HEK293T cells and zebrafish larvae

Xiaoyang Wang [a,b], Shengying Lin [a,b], Roy Wai-Lun Tang [a,b], Hung Chun Lee [a,b], Ho-Hin Chan [b], Sheyne S.A. Choi [b], Ka Wing Leung [a,b], Sarah E. Webb [b], Andrew L. Miller [b], Karl Wah-Keung Tsim [a,b,*]

[a] Center for Chinese Medicine, Clear Water Bay, Kowloon, Hong Kong, China
[b] State Key Laboratory of Molecular Neuroscience, Division of Life Science, The Hong Kong University of Science and Technology, Clear Water Bay, Kowloon, Hong Kong, China

ARTICLE INFO

Keywords:
SARS-CoV-2
Traditional Chinese Medicine
Polygoni Multiflori Radix
S-protein ELISA
3CL protease
Pseudovirus tests

ABSTRACT

Background: Globally, COVID-19 has caused millions of deaths and led to unprecedented socioeconomic damage. There is therefore, in addition to vaccination, an urgent need to develop complementary effective treatments and/or protective and preventative therapies against this deadly disease.

Methods: Here, a multi-component testing platform was established to screen a library of herbal extracts from traditional Chinese medicine (TCM), to identify potent herbal extracts/phytochemicals as possible therapeutics for COVID-19. We utilized assays for spike protein (S-protein) binding to angiotensin-converting enzyme II (ACE2); the enzymatic inhibition of 3CL protease; and entry of the SARS-CoV-2 pseudovirus into cultured HEK293T cells and zebrafish larvae.

Results: Over a thousand herbal extracts were screened and approximately 20 positive hits were identified. Among these, we found that the water and ethanol extracts of Polygoni Multiflori Radix (PMR) significantly inhibited S-protein binding to ACE2, 3CL protease activity, and viral entry into the cell and fish models. The water extract was more effective than the ethanol extract, with IC_{50} values of 25 to 500 μg/ml. In addition, the polysaccharide-depleted fraction of the former, and epigallocatechin gallate (EGCG) which was found in both extracts, displayed significant antiviral activity.

Conclusions: Our results indicate that the water and ethanol extracts of PMR have an inhibitory effect on SARS-CoV-2 pseudovirus host-cell entry. Furthermore, EGCG might be an active component of PMR, which blocks SARS-CoV-2 entry to cells. Taken together, our findings suggest that PMR might be considered as a potential treatment for COVID-19.

Introduction

As of December 2021, the COVID-19 pandemic (caused by variants of SARS-CoV-2) has resulted in more than 270 million confirmed cases and caused over 5 million deaths since its outbreak in December 2019. In India, the largest number of daily confirmed cases has reached 400,000 (World Health Organization, 2021, https://covid19.who.int/, accessed on 15/12/2021). These figures clearly indicate the highly contagious nature of the virus, which has caused a public health emergency, as well as unprecedented damage to the global economy. Despite various COVID-19 vaccines having been approved for public use, which are effective in preventing the most life-threatening symptoms, 100%

Abbreviations: ACE2, Angiotensin-converting enzyme II; ELISA, Enzyme-Linked ImmunoSorbent Assay; EGCG, Epigallocatechin gallate; HEK, Human embryonic kidney fibroblast cells; HPLC, High performance liquid chromatography; HKCMMS, Hong Kong Chinese Medicine Medica Standards; IC_{50}, Half maximal inhibitory concentration; PDB, Protein data bank; PEG, Polyethylene glycol; Polysaccharide-enriched fraction, PS_{enrich}; Polysaccharide-depleted fraction, $PS_{deplete}$; PMR, Polygoni Multiflori Radix; RBD, Receptor binding domain; RT-PCR, Reverse transcription polymerase chain reaction; TCM, Traditional Chinese Medicine; THSG, 2,3,5,4′-tetrahydroxystilbene-2-O-β-D-glucoside.

* Corresponding author at: Center for Chinese Medicine, Division of Life Science, The Hong Kong University of Science and Technology, Clear Water Bay, Hong Kong, China.

E-mail address: botsim@ust.hk (K.W.-K. Tsim).

https://doi.org/10.1016/j.phymed.2022.154154
Received 26 January 2022; Received in revised form 27 April 2022; Accepted 4 May 2022
Available online 9 May 2022

protection cannot be guaranteed especially with the emergence of new viral variants. In addition, in some cases the vaccines themselves have been reported to have a variety of side effects. As such, there is still an urgent need for the development of potent non-vaccine-based therapies against this deadly disease (Liu and Wang et al., 2021; Mulligan et al., 2020).

Since the start of the pandemic, much has been discovered about the route of entry and infection of SARS-CoV-2 virus. Both endosomal and non-endosomal pathways are reported to be involved in the viral entry mechanism, although the former is considered the main route. During infection by SARS-CoV-2, the spike (S) protein of the virus recognises angiotensin-converting enzyme 2 (ACE2) on the host cell surface, and this triggers viral entry *via* endocytosis (Shang et al., 2020; Wang et al., 2020). Once inside the host cells, non-structural proteins, such as 3CL protease, enable viral replication and proliferation, leading to the widespread pathogenic damage of characteristic of this disease (Bristow et al., 2020). In view of this entry and replication mechanism, several proteins (including ACE2, S-protein and 3CL protease) have been identified as potential drug targets for the prevention and/or treatment of COVID-19. As an anti-COVID-19 strategy, small molecules that bind one or more of these proteins, inhibit the route of SARS-CoV-2 entry into cells, and/or disrupt the downstream biological activities of the virus should be identified (Prasansuklab et al., 2021).

In China, traditional Chinese medicine (TCM) has been reported to have good efficacy in the clinical treatment of viral infections. Indeed, in 2003, when SARS-CoV-1 began to threaten public health, several TCM products were identified to effectively relieve the symptoms, reduce the number of fatalities, and prevent the course of the disease (Yang et al., 2020). Today in China, more than ten prescriptions containing TCM have been recommended by clinics for the treatment of mild and moderate cases of COVID-19. Their promising efficacy has inspired the search for other novel TCMs as potential treatments for this disease (Wang et al., 2021).

Here, we established a screening platform for anti-SARS-CoV-2 infection by testing the ability of an extensive library of TCM herbs/single molecules to inhibit the S-protein-ACE2 interaction, 3CL protease activity, and/or viral entry into cells and zebrafish (*Danio rerio*) larvae. From the 1,000 herbal extracts screened, $>$ 20 positive hits were identified. Among these, the water and ethanol extracts of Polygoni Multiflori Radix (PMR) yielded significant inhibition of SARS-CoV-2 host-cell entry. PMR is a well-established TCM, which has previously been utilized for the treatment of various diseases, including cancer, liver cirrhosis and hair loss. The major phytochemicals in PMR are stilbenes, quinones, and flavonoids (Ho et al., 2007; Lee et al., 2015). Here, we demonstrate that the water and ethanol extracts of PMR are non-toxic, and they significantly inhibit the S-protein/ACE2 interaction, 3CL protease activity, and viral entry into both HEK293T cells and zebrafish larvae. As such, they are strong contenders for a more in-depth analysis prior to utilizing the live virus in mammalian models, with a view for potential drug development and/or clinical application.

Materials and methods

Cell culture

HEK293T cells (American Type Culture Collection, Manassas, VA, USA) were maintained in high glucose Dulbecco's Modified Eagle Medium (DMEM) supplemented with 1% penicillin/streptomycin and 10% fetal bovine serum (Thermo Fisher Scientific, Waltham, MA, USA; herein called culture medium) at 37 °C in an incubator with water-saturated atmosphere and 5% CO_2. Fresh culture medium was supplied every other day. HEK293T cells overexpressing hACE2 (human ACE2) were prepared by transfection with the pcDNA3.1-hACE2 plasmid (Addgene, Watertown, MA, USA). The cell viability was determined as described previously (Wu et al., 2019).

Herbal extract preparation

PMR powder (10.0 g), grounded from roots of *Polygonum multiflorum* Thunb., was placed in a 250-ml round-bottomed flask and dissolved in 100 ml 90% ethanol or distilled water. The solutions were refluxed for 1 h before being filtered through a paper filter (Advantec, Tokyo, Japan). These were then evaporated to dryness with a rotary evaporator to yield final ethanol (PMR_{EtOH}) and water (PMR_{water}) extracts of 2.05 g and 4.16 g, respectively. To fractionate the PMR_{water}, 0.64 g of this extract was dissolved in 10 ml water and then added to 40 ml EtOH. The mixture was stored at 4 °C for 16 h, then centrifuged at 7,000 rpm for 15 min and filtered through a paper filter (Advantec). The precipitate was washed twice with 20 ml water and dried to yield a polysaccharide-enriched fraction (PS_{enrich}) of $\sim$ 32 g, whereas the filtrate was evaporated to dryness with a rotary evaporator to yield a polysaccharide-depleted fraction ($PS_{deplete}$) of $\sim$ 0.23 g.

Carbohydrate determination

In accordance with a well-established methodology of colourimetry (HKCMMS; Hong Kong Chinese Medicine Medica Standards, 2008), $PS_{deplete}$ or PS_{enrich} (40 mg) was dissolved in 50 ml boiling water in a 50-ml volumetric flask. Three ml of this solution was added to another 50-ml volumetric flask and diluted 10 times. Two ml of this solution was then added to a 10-ml tube and 6 ml of anthrone sulphuric acid solution was added. The mixture was cooled on ice for 15 min and then the absorbance was measured at 625 nm.

HPLC analysis

HPLC detection and calculation were conducted according to methods developed by the HKCMMS utilising PMR_{EtOH} (1 mg/ml), PMR_{water} (1 mg/ml), PS_{enrich} (1 mg/ml), $PS_{deplete}$ (1 mg/ml), 2,3,5,4′-tetrahydroxystilbene-2-O-β-D-glucoside (THSG, 0.1 mg/ml), emodin (0.1 mg/ml), physcion (0.1 mg/ml) and EGCG (0.1 mg/ml) (all at purity $>$ 95% from Chengdu Must, Chengdu, China). The HPLC gradient comprised 8% acetonitrile for 0-5 min, 8-20% acetonitrile for 5-15 min, 20% acetonitrile for 15-35 min, and 20-30% acetonitrile for 35-45 min. The detection wavelength was 230 nm.

SARS-CoV-2 pseudotyped-virus production

HEK293T cells at 80% confluence were transfected with components of SARS-Related Coronavirus 2, Wuhan-Hu-1 Spike-Pseudotyped Lentiviral Kit (NR-52948; BEI Resources, NIAID, Bethesda, MD, USA), including SARS-CoV-2 Spike Glycoprotein (NR-52514), lentiviral backbone expressing *Luciferase* and *ZsGreen* (NR-52516), and helper plasmids (NR-52517, NR-52518, NR-52519) using Lipofectamine™ 3000 (Thermo Fisher Scientific) or JetPRIME (Polyplus, Shangai, China) transfection reagent, according to the manufacturers' instructions. After 72 h, the SARS-CoV-2 pseudotyped-virus particles (hereafter called pseudovirus) were collected and passed through a 0.45 μm filter. In most HEK293T cell-based experiments, the pseudovirus was used directly. For the zebrafish experiments, the pseudovirus was subsequently purified using polyethylene glycol (PEG; hereafter called PEG-pseudovirus; Lo and Yee, 2007), and the culture medium was replaced with phosphate buffered saline (PBS; 137 mM NaCl, 2.7 mM KCl, 10 mM Na_2HPO_4, 1.8 mM KH_2PO_4 pH 7.4). The pseudovirus and PEG-pseudovirus were stored at -80°C until required.

Inhibiting SARS-CoV-2 pseudovirus entry in HEK293T cells

ACE2-overexpressing HEK293T cells were seeded into 48-well plates, after which 400 μl culture medium containing SARS-CoV-2 pseudovirus (100 μl) and PMR_{EtOH} or PMR_{water} (at various concentrations) were added, and they were incubated at 37 °C for 24 h. This

medium was then replaced with fresh medium, and the cells allowed to recover for 48 h. The cells were washed with PBS just before the luciferase assay. PMR_{EtOH}, PMR_{water}, PS_{enrich} and $PS_{deplete}$ were tested at final concentrations of 1, 10, 25, 50, and 100 μg/ml, whereas EGCG was tested at 10, 25, 50, 75 and 100 μM. An anti-SARS-CoV-2 neutralizing antibody (at 1 μg/ml; A19215, ABClonal, Woburn, MA, USA) was used as a positive control, whereas a solvent blank without the pseudovirus was used as a negative control. The inhibition percentage was determined according to the luciferase activity normalized to the luciferase activity without PMR treatment.

Luciferase assay

The luciferase assay was conducted as previously described (Wu et al., 2019). The percentage inhibition of each sample was calculated as follows: Inhibition rate = (Luciferase activity of the solvent blank − Luciferase activity of the sample) / (Luciferase activity of the solvent blank − Luciferase activity of group without pseudovirus) × 100%.

Screening spike protein inhibitors

Spike protein inhibition was analysed with SARS-CoV-2 Spike-ACE2 Binding Assay kit (ImmunoDiagnostics Ltd. Hong Kong, China) according to the manufacturer's instructions. The reaction was terminated by adding 2 M H_2SO_4, and a FlexStation 3 microplate reader (Molecular Devices, San Jose, CA, USA) was used to quantify the data. The percentage of inhibition was calculated as follows: Percentage of inhibition = $(P_{Avg} - S_{Avg}) / P_{Avg} \times 100\%$, where P_{Avg} and S_{Avg} are the mean OD values of the positive control and test sample, respectively.

Screening 3CL protease inhibitors

Extracts were tested for binding 3CL protease on a fluorogenic substrate with the SensoLyte SARS-CoV-2 3CL Protease Activity assay kit (AnaSpec, San Jose). The 3CL protease bound with the substrate emitted fluorescence at 460 nm when using a 360 nm excitation wavelength. The percentage of Inhibition was calculated as follows: Percentage of inhibition = $(P_{Avg, b} - S_{Avg, b}) / P_{Avg, b} \times 100\%$, where $P_{Avg, b}$ and $S_{Avg, b}$ are the mean fluorescence of the positive control and test sample, respectively, subtracted from the mean fluorescence of the blank.

Inhibiting pseudovirus entry in zebrafish

Zebrafish larvae at 3 days post-fertilization (dpf) were treated for 6 h with Danieau's solution (Westerfield, 2000) ± 125 μg/ml PMR_{water}, or with Danieau's solution containing 0.1% DMSO ± 30 μg/ml PMR_{EtOH} in a 24-well plate (SPL Life Sciences, Gyeonggi-do, Korea). Each experiment was conducted using 10 embryos *per* treatment group, and repeated $n = 4$. The larvae were then transferred to 96-well plates, one larva *per* well, containing the respective treatment solution plus 8 μl PEG-pseudovirus, incubated at 28 °C for 72 h, until they reached ~ 6.25 dpf. The larvae from each treatment group were pooled and washed with Milli-Q water for 6 × 20 min with gentle agitation prior to RNA extraction.

RNA extraction, reverse transcription, and RT-PCR

RNA extraction and reverse transcription were conducted as described (Kelu et al., 2017). The converted cDNA was then amplified, for 35 cycles, by PCR using 2 × Rapid Taq Master Mix (Vazyme Biotech, Nanjing, China), after which the PCR products were separated on a 2% agarose gel. The band intensities were quantified using ImageJ (NIH; https://imagej.nih.gov/ij/). The level of expression of luciferase (Luc) mRNA was determined against that of glucose-6-phosphate dehydrogenase (g6pd) mRNA, and the expression levels following treatment with PMR_{water} or PMR_{EtOH} were measured. The primers used were as follows: *g6pd*-Fwd: 5' TGC TTC CAC CAG CTC TGA TG 3'; *g6pd*-Rev: 5' CCC TCA ACT CAT CAC TGC GT 3'; *Luc*-Fwd: 5' AAA CGC TTC CAC CTA CCA GG 3'; *Luc*-Rev: 5' TCC ACG ATC TCC TTC TCG GT 3'.

Computational docking analysis

The chemical structures of phytochemicals were downloaded from Pubchem (https://pubchem.ncbi.nlm.nih.gov/), and the S-protein structure was downloaded from the Protein Data Bank (https://www.rcsb.org/). Virtual screening was performed with SEESAR (Version 11.0, https://www.biosolveit.de/) as follows: (i) The binding site was determined according to the residues forming the identified druggable pocket. Ligand binding states including protonation and tautomeric forms were subsequently evaluated using the ProToss method to generate the most accessible hydrogen network. (ii) Docking modulation was performed using the "Compute LeadIT Docking" mode in the FlexX algorithm; ten binding conformations for each ligand were generated. (iii) The binding energy (i.e., ΔG) and estimated HYDE affinity (KiHYDE) for each ligand pose were calculated using the "Assess Affinity with HYDE in SEESAR" mode in the HYDE rescoring function (Spagnolli et al., 2021).

Results

PMR extracts on S-protein binding and 3CL protease activity

In our HPLC analysis, THSG, emodin, physcion and EGCG were utilised as standard markers of the PMR extracts (Fig. 1). PMR_{water}

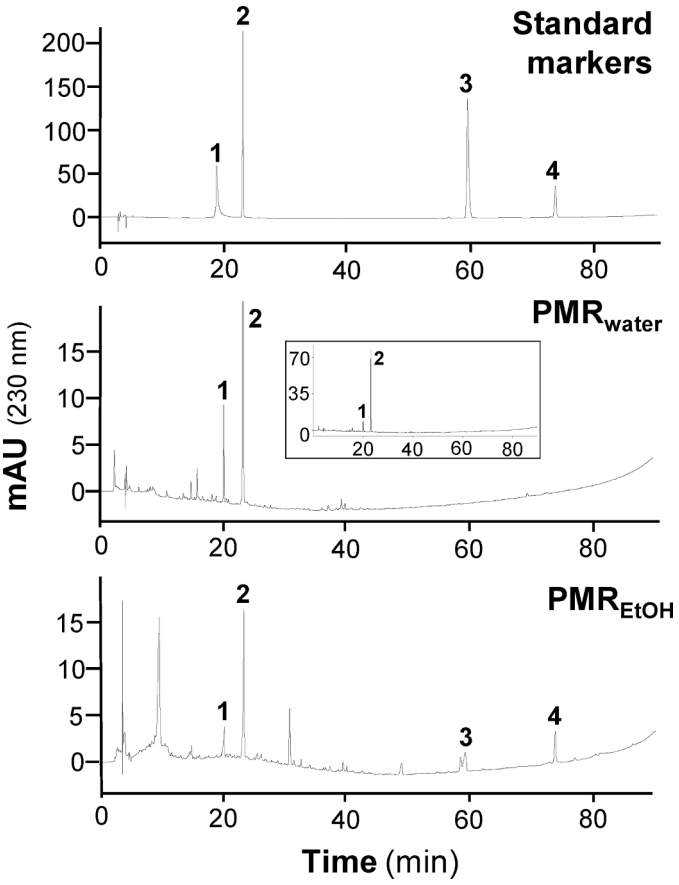

Fig. 1. HPLC chromatograms of the PMR extracts. The characteristic peaks of mixed standard markers, and those found in PMR_{water} and PMR_{EtOH}, which were revealed at an absorbance of 230 nm. Insert shows data at higher mAU. 1: EGCG; 2: THSG; 3: emodin; 4: physcion.

consisted of 5.5% THSG, 0.03% emodin, 0.02% physcion and 0.71% EGCG, whereas PMR_{EtOH} contained 1.86% THSG, 0.80% emodin, 0.58% physcion and 0.37% EGCG. The extractive efficacy was 41.6% for PMR_{water} and 20.5% for PMR_{EtOH}. These parameters served as quality controls for subsequent experiments.

An ELISA was utilised to test the binding of S-protein to ACE2. Initially, a standard inhibitor (calibrated to NIBSC code 20/136), provided by the supplier, was tested as a positive control (Fig. 2**A**). The inhibitor blocked binding to S-protein in a dose-dependent manner. To investigate the binding activity between the PMR extracts and S-protein, PMR_{water} or PMR_{EtOH} were tested at various concentrations up to 2.5 mg/ml. Both extracts inhibited the binding in a dose-dependent manner (Fig. 2**B**), with an estimated IC_{50} of ~ 1 to 2 mg/ml.

We also tested the effects of PMR extracts on enzymatic activity of 3CL protease. We used GC-376 as a positive control, which has a broad-spectrum of anti-viral effects (Hu et al., 2021). As shown in Fig. 3, PMR_{water} and PMR_{EtOH} inhibited 3CL protease activity in a dose-dependent manner, with IC_{50} values of ~ 0.25 mg/ml and ~ 0.5 mg/ml, respectively. Interestingly, PMR_{water} displayed a higher maximal inhibition rate than PMR_{EtOH}, i.e., ~ 100% versus ~ 70% inhibition.

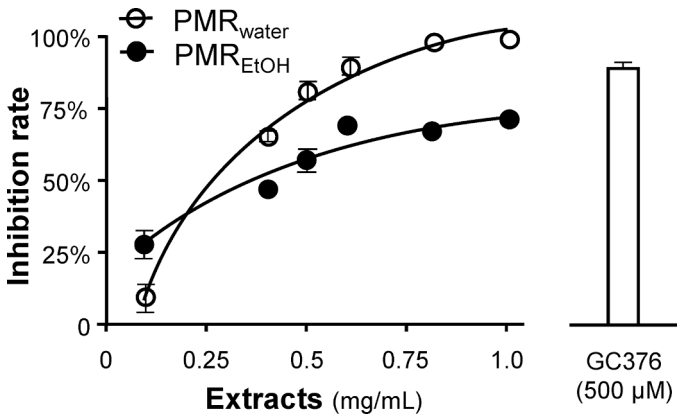

Fig. 3. Inhibition of 3CL protease activity. PMR_{water} and PMR_{EtOH} inhibited the activity of 3CL protease of SARS-CoV-2 in a dose-dependent manner. A control inhibitor, GC-376 (500 μM), was used as a positive control. The inhibition percentage was determined according to the optical density normalized to the 3CL protease activity without extract. The data represent mean ± SD (n = 3).

PMR extracts on viral entry

As the S-protein and 3CL protease results indicated that the PMR extracts might prevent viral entry into host cells, we investigated the effect of PMR_{water} and PMR_{EtOH} on the entry of a *Luc*-expressing SARS-Cov-2 pseudovirus into ACE2-overexpressing HEK293T cells. The luciferase-generated luminescence was quantified to determine the amount of virus entering the cells. The luminescence decreased as the

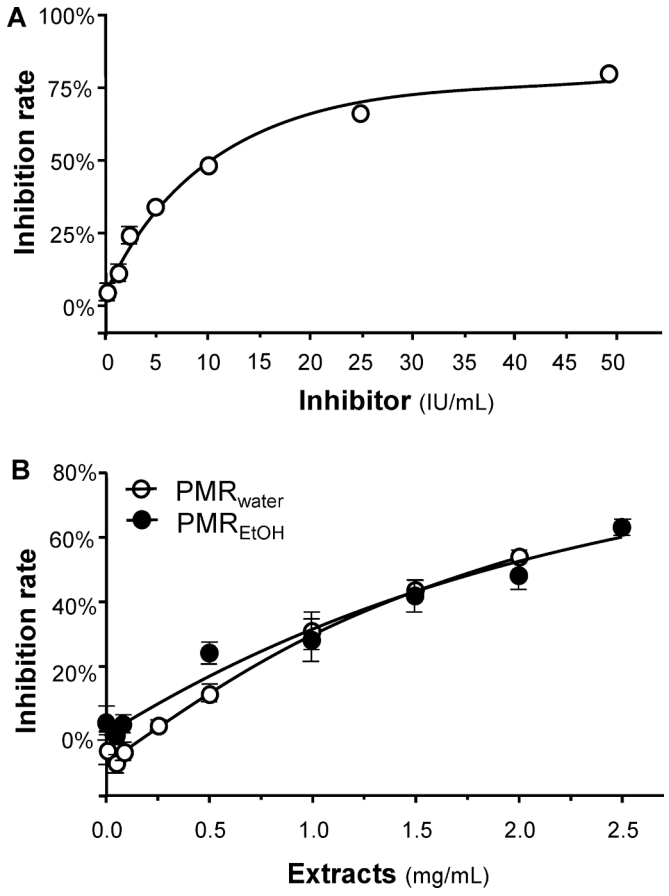

Fig. 2. Inhibition of S-protein-hACE2 binding. S-protein-hACE2 binding was analysed by ELISA. (A) Line graph showing the response of a standard inhibitor (calibrated to NIBSC code 20/136), which was used as a positive control. (B) S-protein-hACE2 binding was inhibited by PMR_{water} and PMR_{EtOH} in a dose-dependent manner. The inhibition percentage was determined from the binding signal normalized to the interaction between spike RBD and hACE2 without extract. The data represent mean ± SD (n = 3).

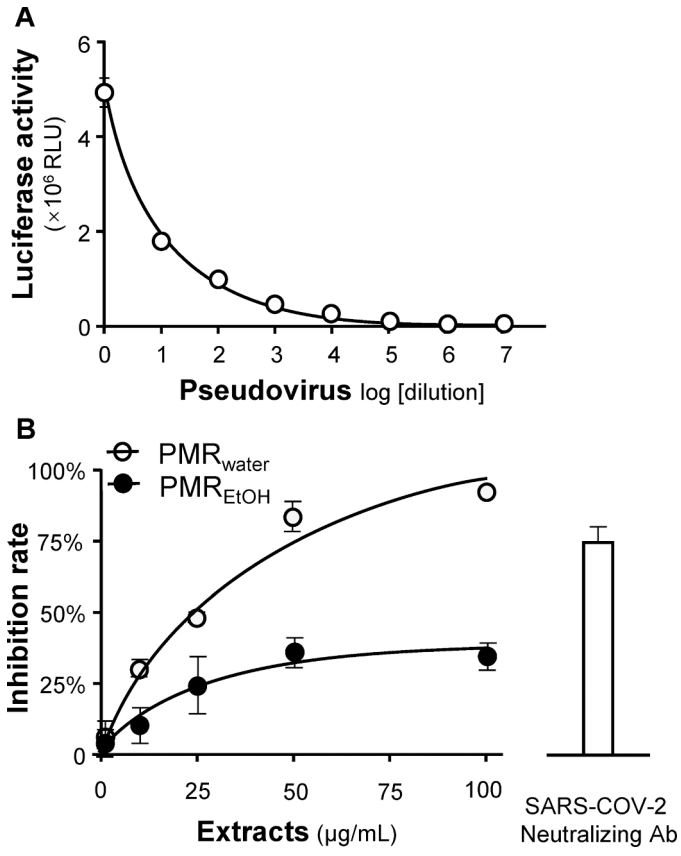

Fig. 4. Inhibition of pseudovirus entry into HEK293T cells overexpressing hACE2. (A) The amount of intracellular luciferase activity (indicating the rate of virus entry) was measured at different dilutions of the pseudovirus. (B) Pseudovirus entry was inhibited by PMR_{water} or PMR_{EtOH} in a dose-dependent manner. The inhibition percentage was determined according 20 to the luciferase activity normalized to the luciferase activity without extract. A SARS-CoV-2 neutralizing antibody was used as a positive control. The data represent mean ± SD, (n = 3).

pseudovirus was diluted, indicating the efficacy of the assay (Fig. 4A). An anti-SARS-CoV-2 neutralising antibody (positive control) inhibited total pseudoviral entry by ~ 75%. Furthermore, PMR_{water} or PMR_{EtOH} inhibited pseudoviral entry in a dose-dependent manner (Fig. 4B). However, maximal inhibition was only achieved by PMR_{water}, which displayed ~ 3-fold higher effectiveness than PMR_{EtOH}. Neither extract affected the cell viability up to 100 μg/ml (**Supplementary Fig. S1**).

The expression of the *Luc* gene was used as an indicator of successful PEG-pseudovirus entry in zebrafish larvae. The 3-day-old larvae were pre-treated with PMR_{water} or PMR_{EtOH} for 6 h before being treated with either of these extracts plus PEG-pseudovirus for a further 72 h. Both extracts significantly inhibited the expression of *Luc* when compared with the respective untreated and DMSO controls (Fig. 5A&B). These results suggest that both extracts can prevent pseudovirus entry into zebrafish larvae.

Identification of active fractions of PMR extract

Due to its higher potency, PMR_{water} was selected for further fractionation. Thus, it was subjected to EtOH precipitation to obtain PS_{enrich} and $PS_{deplete}$. We found that most of our selected marker chemicals from PMR_{water} remained in $PS_{deplete}$ (Fig. 6A), and that PS_{enrich} contained > 86% carbohydrate, of which > 75% were polysaccharides with molecular weights > 10 kDa (Fig. 6B). In the pseudoviral entry assay, $PS_{deplete}$ was more potent than PMR_{water} in blocking viral entry, with an IC_{50} value of ~ 15 μg/ml (Fig. 7A). Indeed, maximal blocking was revealed by $PS_{deplete}$ alone.

The enriched chemicals within $PS_{deplete}$ were also tested using the viral entry assays. Several phytochemicals (e.g., THSG, emodin and EGCG) were enriched in PMR_{water} (Sun et al., 2018; Yi et al., 2007). Of these, EGCG inhibited pseudovirus entry robustly in a dose-dependent manner, exhibiting complete inhibition at ~ 100 mM and an IC_{50} at ~ 30 mM (Fig. 7B). As PMR_{water} contained higher amounts of EGCG than PMR_{EtOH} (0.71% *vs* 0.37%), this might account for the different

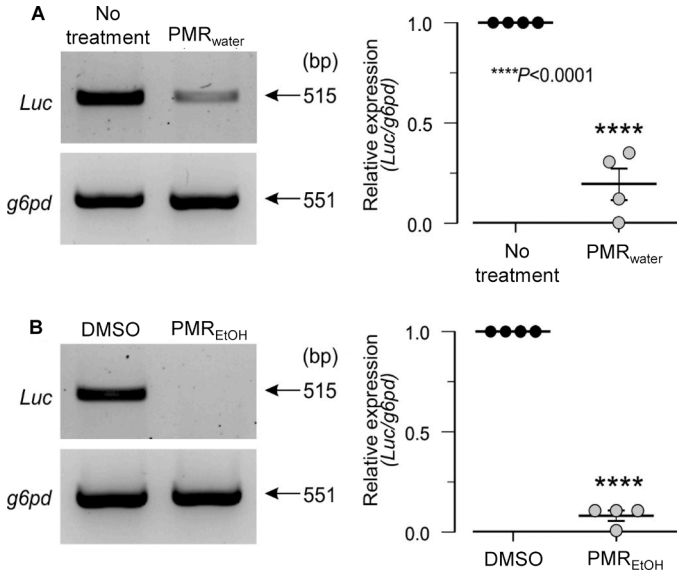

Fig. 5. PMR_{water} and PMR_{EtOH} inhibit the entry of SARS-CoV-2 PEG-pseudovirus in zebrafish. Larvae at 3 dpf were pre-treated with (A) PMR_{water} or (B) PMR_{EtOH}, then co-treated with the respective extract and SARS-CoV-2 PEG-pseudovirus for a further 72 h. PCR amplification of whole larval cDNA showed the relative level of Luc expression in the treatment and control groups (left). The relative level of Luc expression was quantified by normalization to the expression level of g6pd (right). The data show that treatment with PMR_{water} or PMR_{EtOH} inhibited the expression of Luc (and thus the entry of PEG-pseudovirus) in larvae. The data represent the mean ± SD (n = 4), and statistical differences were tested using the 2-sample ttest, ****p < 0.0001.

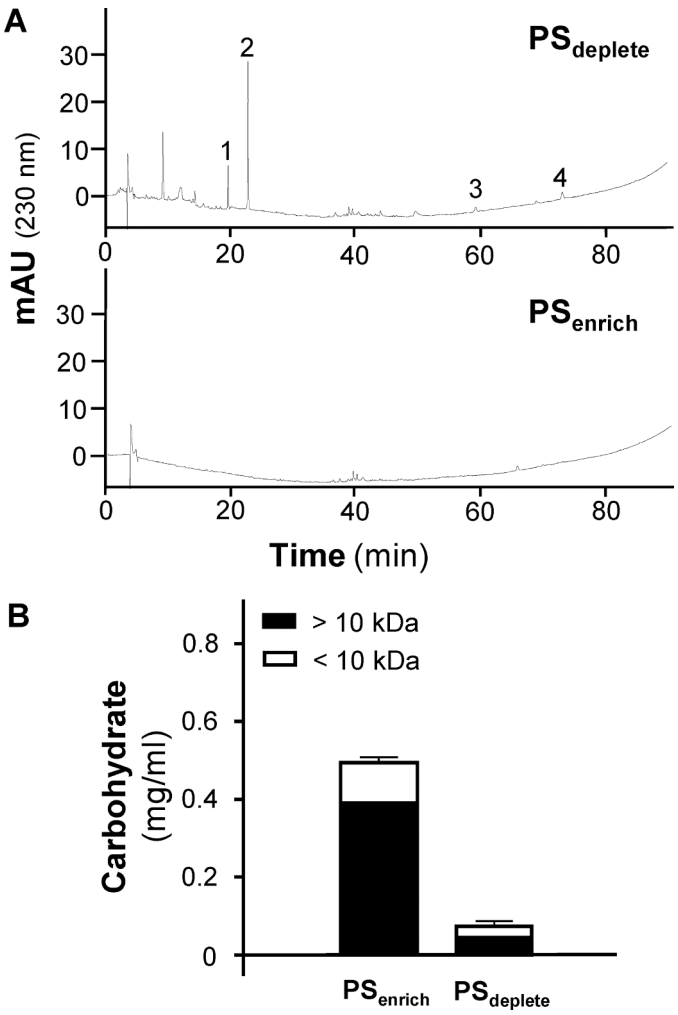

Fig. 6. Fractionation of PS_{enrich} and $PS_{deplete}$. (A) HPLC analyses of both fractions, at 1 mg/ml, were revealed at 230 ± 4 nm. EGCG (1), THSG (2), emodin (3) and physcion (4) are marked. (B) $PS_{deplete}$ and PS_{enrich} (0.5 ml each at 1 mg/ml dried weight) were transferred to a 10 kDa cut-off concentrator (Sartorius, German) and centrifuged at 14,000 g for 15 min. The carbohydrate content was measured with phenol-sulfuric acid. The values are expressed as mean ± SD, n = 3.

levels of performance of these extracts in the antiviral assays. Compared with EGCG, the other PMR phytochemicals tested, exhibited no significant effects on viral entry (**Supplementary Fig. S2**). To further validate our hypothesis, the receptor binding domain (RBD) of the S-protein was selected as a binding site for docking analysis. The RBD inhibitor K22 (Xiu et al., 2020), was predicted to bind RBD with a binding energy of -12 kJ/mol. In comparison, EGCG was found to bind the RBD with an energy of -7.5 kJ/mol, whereas no significant binding activity was observed for the other PMR chemicals (**Supplementary Fig. S3A**). As testing platforms based on the omicron variant of SARS-CoV-2 were not available to our research team, the effect of EGCG on this variant was evaluated by computational docking (**Supplementary Fig. S3B**). Interestingly, EGCG was predicted to require less energy to bind to this variant than to the wildtype virus (i.e., -15.2 *vs* -7.5 kJ/mol). This suggests that EGCG, and its parental TCM herb, PMR, might also have potent antiviral effects with regards to the omicron variant of SARS-CoV-2.

Discussion

Given that COVID-19 has caused (and is still causing) so many deaths

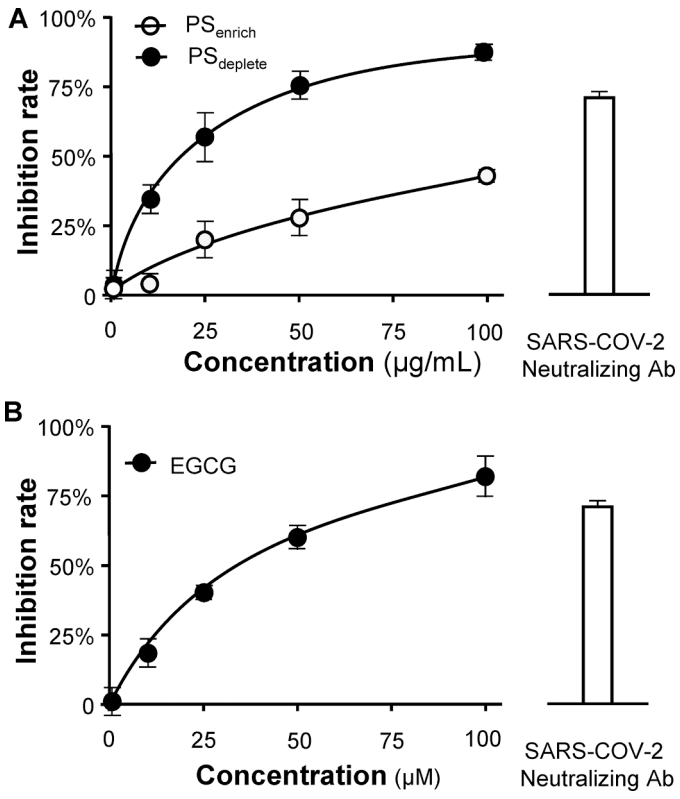

Fig. 7. Inhibition of pseudovirus entry by PS_{enrich}, $PS_{deplete}$ and EGCG. Pseudovirus entry in hACE2-overexpressing HEK293T cells were inhibited by (A) PS_{enrich} and $PS_{deplete}$, and (B) EGCG, all in a dose-dependent manner. The data represent mean ± SD, ($n = 3$). A SARSCoV-2 neutralizing antibody was used as the positive control.

globally, there is an urgent need to find novel treatments that are protective against and/or that can treat the symptoms of SARS-CoV-2 infection. TCM is a rich source of herbs/phytochemicals that can be exploited in the search for novel drug candidates. In China, some TCMs are reported to have good efficacy in the clinical treatment of different viral infections, and so these are being recruited in the fight against COVID-19. For example, an herbal decoction called *Qingfei Paidu* (consisting of Dioscoreae Rhizoma, Aurantii Immaturus Fructus, Poria and others) has been formally recognised in China as one of the first-line treatments against COVID-19. *Huoxiang Zhengqi* (containing 10 TCM herbs including Atractylodis Rhizoma, Citri Reticulata Pericarpium, Magnoliae Officinalis Cortex, and Angelicae Dahuricae Radix), is also being used to treat this disease (Al-Romaima et al., 2020; Luo et al., 2020). Thus, other TCMs might also prove to be promising therapies for the prevention and treatment of COVID-19.

Polygonum plants are a family of herbs that have good anti-viral properties (Sun et al., 2018). Taking *P. perfoliatum* L. as an example, the herbal extract and its corresponding chemical, quercetin-3-O-β-D-glucuronide, has been reported (through *in vivo* studies) to inhibit influenza A virus (Fan et al., 2011). Our new results also demonstrate the antiviral properties of *Polygonum*-type TCMs. Like other members of the *Polygonum* family, PMR has long been utilised in medicinal practices against various diseases as it has a good record of safety and effectiveness (Sun et al., 2018). Although the antiviral properties of PMR have not been reported before, the antiviral activity of EGCG against SARS-CoV-2 was reported by Liu and Bodnar et al. (2021). We confirmed the antiviral effects of EGCG in our testing platforms, and suggest that this is one of the active components in our PMR extracts. In addition, as EGCG docked with the S-protein of the omicron SARS-CoV-2 variant with higher binding energy than with the wildtype virus, this suggests that PMR extracts might be highly effective at protecting against omicron infection. However, as the amount of EGCG was relatively low in the PMR extracts (e.g., ~ 0.71% in PMR_{water}), the other phytochemicals might also have antiviral properties.

Conclusion

In conclusion, COVID-19 remains a disease of major concern throughout the world and effective treatments are still urgently required to complement vaccination. Here, we established a dual screening platform comprising various *in vitro* and *in vivo* experimental approaches, to provide a first step in the identification of TCMs with anti-COVID-19 potential. Using this platform, we established that the water and ethanol extracts of PMR were non-toxic and inhibited the S-protein-ACE2 interaction, the activity of 3CL protease, and entry of the SARS-CoV-2 pseudovirus into HEK293T cells and zebrafish larvae. We also found that EGCG is an active component of PMR, and it is responsible for at least some of the antiviral effects of this herb. Taken together, our new findings might promote future studies on the effect of PMR as a potential preventative measure against infection of the active SARS-CoV-2 virus.

Funding

This work was supported by a Health and Medical Research Fund (COVID-19) award (HMRF20SC07[COVID190213]) from the Hong Kong Government Food and Health Bureau; The Key-Area Research and Development Program of Guangdong Province (2020B1111110006); Hong Kong RGC-GFC 16100921; Zhongshan Municipal Bureau of Science and Technology (2019AG035); Guangzhou Science and Technology Committee Research Grant (GZSTI16SC02; GZSTI17SC02); GBA Institute of Collaborate Innovation (GICI-022); Special Project of Foshan University of Science and Technology in 2019 (FSUST19-SRI10); Hong Kong RGC Theme-based Research Scheme (T13-605/18-W); Hong Kong Innovation Technology Fund (PRP/076/20FX; PRP/076/20FX; UIM/385, ITS/500/18FP; ITCPD/17-9); TUYF19SC02, PD18SC01 and HMRF18SC06; HMRF20SC07; AFD20SC01; and Shenzhen Science and Technology Innovation Committee (ZDSYS201707281432317).

Ethics approval

All the procedures used with zebrafish in this study were conducted in accordance with the guidelines and regulations outlined by the Animal Ethics Committee of HKUST, and the Department of Health, Hong Kong.

CRediT authorship contribution statement

Xiaoyang Wang: Methodology. **Shengying Lin:** Software, Writing – original draft. **Roy Wai-Lun Tang:** Investigation. **Hung Chun Lee:** Investigation. **Ho-Hin Chan:** Investigation. **Sheyne S.A. Choi:** Methodology. **Ka Wing Leung:** Project administration. **Sarah E. Webb:** Project administration, Writing – review & editing. **Andrew L. Miller:** Conceptualization, Supervision, Writing – review & editing. **Karl Wah-Keung Tsim:** Conceptualization, Supervision, Writing – review & editing.

Declaration of Competing Interest

The authors declare that there is no conflict of interest associated with this publication.

Acknowledgments

We thank Prof. Jonathan S. Marchant (Medical College of Wisconsin, USA) for providing us with the SARS-related Coronavirus 2 lentiviral kit and ACE2 plasmid.

Supplementary materials

Supplementary material associated with this article can be found, in the online version, at doi:10.1016/j.phymed.2022.154154.

References

Al-Romaima, A., Liao, Y., Feng, J., Qin, X., Qin, G., 2020. Advances in the treatment of novel coronavirus disease (COVID-19) with Western medicine and traditional Chinese medicine: a narrative review. J. Thorac. Dis. 10, 6054–6069.

Bristow, M.R., Zisman, L.S., Altman, N.L., Gilbert, E.M., Lowes, B.D., Minobe, W.A., Slavov, D., Schwisow, J.A., Rodriguez, E.M., Carroll, I.A., Keuer, T.A., Buttrick, P.M., Kao, D.P., 2020. Dynamic regulation of SARS-CoV-2 binding and cell entry mechanisms in remodeled human ventricular myocardium. JACC Basic Transl. Sci. 9, 871–883.

Fan, D., Zhou, X., Zhao, C., Chen, H., Zhao, Y., Gong, X., 2011. Anti-inflammatory, antiviral and quantitative study of quercetin-3-O-β-D-glucuronide in *Polygonum perfoliatum L*. Fitoterapia 6, 805–810.

HKCMS office, 2008. Hong Kong Chinese Medicine Medica standards. Polygoni Multiflori Radix, 2nd ed. Department of Health, The Government of Hong Kong Special Administrative Region.

Ho, T., Wu, S., Chen, J., Li, C., Hsiang, C., 2007. Emodin blocks the SARS coronavirus spike protein and angiotensin-converting enzyme 2 interaction. Antivir. Res. 2, 92–101.

Hu, Y., Ma, C., Szeto, T., Hurst, B., Tarbet, B., Wang, J., 2021. Boceprevir, calpain inhibitors II and XII, and GC-376 have broad-spectrum antiviral activity against coronaviruses. ACS Infect. Dis. 7, 586–597.

Kelu, J.J., Webb, S.E., Parrington, J., Galione, A., Miller, A.L., 2017. Ca2+ release *via* two-pore channel type 2 (TPC2) is required for slow muscle cell myofibrillogenesis and myotomal patterning in intact zebrafish embryos. Dev. Biol. 425, 109–129.

Lee, B., Lee, K., 2015. Discrimination and proper use of polygoni multiflori radix, cynanchi wilfordii radix, and cynanchi auriculati radix in Korea: a descriptive review. Evid-Based Compl. Alt. 2015 https://doi.org/10.1155/2015/827380.

Liu, J., Bodnar, B.H., Meng, F, Khan, A.I., Wang, X., Saribas, S., Wang, T., Lohani, S.C., Wang, P., Wei, Z., Luo, J., Zhou, J., Wu, J., Luo, G., Li, Q., Hu, W., Ho, W., 2021. Epigallocatechin gallate from green tea effectively blocks infection of SARS-CoV-2 and new variants by inhibiting spike binding to ACE2 receptor. Cell Biosci. 11, 168–182.

Liu, J., Wang, J., Xu, J., Xia, H., Wang, Y., Zhang, C., Chen, W., Zhang, H., Liu, Q., Zhu, R., Shi, Y., Shen, Z., Xing, Z., Gao, W., Zhou, L., Shao, J., Shi, J., Yang, X., Deng, Y., Wu, L., Lin, Q., Zheng, C., Zhu, W., Wang, C., Sun, Y.E., Liu, Z., 2021. Comprehensive investigations revealed consistent pathophysiological alterations after vaccination with COVID-19 vaccines. Cell Discov. 1, 99–113.

Lo, H.L., Yee, J.K., 2007. Production of vesicular stomatitis virus G glycoprotein (VSV-G) pseudotyped retroviral vectors. Curr. Protoc. Hum. Genet. 52, 12.7.1–12.7.11.

Luo, H., Gao, Y., Zou, J., Zhang, S., Chen, H., Liu, Q., Tan, D., Han, Y., Zhao, Y., Wang, S., 2020. Reflections on treatment of COVID-19 with traditional Chinese medicine. Chin. Med. 15 https://doi.org/10.1186/s13020-020-00375-1.

Mulligan, M.J., Lyke, K.E., Kitchin, N., Absalon, J., Gurtman, A., Lockhart, S., Neuzil, K., Raabe, V., Bailey, R., Swanson, K.A., Li, P., Koury, K., Kalina, W., Cooper, D., Fontes-Garfias, C., Shi, P.-Y., Tureci, O., Tompkins, K.R., Walsh, E.E., Frenck, R., Falsey, A. R., Dormitzer, P.R., Gruber, W.C., Sahin, U., Jansen, K.U., 2020. Phase I/II study of COVID-19 RNA vaccine BNT162b1 in adults. Nature 7830, 589–593.

Prasansuklab, A., Theerasri, A., Rangsinth, P., Sillapachaiyaporn, C., Chuchawankul, S., Tencomnao, T., 2021. Anti-COVID-19 drug candidates: a review on potential biological activities of natural products in the management of new coronavirus infection. J. Tradit. Complement. Med. 2, 144–157.

Shang, J., Wan, Y., Luo, C., Ye, G., Geng, Q., Auerbach, A., Li, F., 2020. Cell entry mechanisms of SARS-CoV-2. Proc. Natl. Acad. Sci. U.S.A. 21, 11727–11734.

Spagnolli, G., Massignan, T., Astolfi, A., Biggi, S., Rigoli, M., Brunelli, P., Libergoli, M., Ianeselli, A., Orioli, S., Boldrini, A., Terruzzi, L., Bonaldo, V., Maietta, G., Lorenzo, N. L., Fernandez, L.C., Codeseira, Y.B., Tosatto, L., Linsenmeier, L., Vignoli, B., Petris, G., Gasparotto, D., Pennuto, M., Guella, G., Canossa, M., Altmeppen, H.C., Lolli, G., Biressi, S., Pastor, M.M., Requena, J.R., Mancini, I., Barreca, M.L., Faccioli, P., Biasini, E., 2021. Pharmacological inactivation of the prion protein by targeting a folding intermediate. Commun. Biol. 4, 62–77.

Sun, L., Wang, M., Zhang, H., Liu, Y., Ren, X., Deng, Y., Qi, A., 2018. Comprehensive analysis of polygoni multiflori radix of different geographical origins using ultra-high-performance liquid chromatography fingerprints and multivariate chemometric methods. J. Food Drug Anal. 1, 90–99.

Wang, H., Xu, B., Zhang, Y., Duan, Y., Gao, R., He, H., Li, X., Li, J., 2021. Efficacy and safety of traditional Chinese medicine in coronavirus disease 2019 (COVID-19): a systematic review and meta-analysis. Front. Pharmacol. https://doi.org/10.3389/fphar.2021.609213.

Wang, Q., Zhang, Y., Wu, L., Niu, S., Song, C., Zhang, Z., Lu, G., Qiao, C., Hu, Y., Yuen, K.-Y., Wang, Q., Zhou, H., Yan, J., Qi, J., 2020. Structural and functional basis of SARS-CoV-2 entry by using human ACE2. Cell 4, 894–904.

Westerfield, M., 2000. The Zebrafish Book. A guide for the laboratory use of zebrafish (*Danio rerio*), 4th ed. University of Oregon Press, Eugene.

World Health Organization. https://covid19.who.int/ (Accessed on 15/12/2021).

Wu, Q.-Y., Wong, Z.C.-F., Wang, C., Fung, A.H.-Y., Wong, E.O.-Y., Chan, G.K.-L., Dong, T. T.-X., Chen, Y., Tsim, K.W.-K., 2019. Isoorientin derived from *Gentiana veitchiorum* Hemsl. flowers inhibits melanogenesis by down-regulating MITF-induced tyrosinase expression. Phytomedicine 57, 129–136.

Xiu, S., Dick, A., Ju, H., Mirzaie, S., Abdi, F., Cocklin, S., Zhan, P., Liu, X., 2020. Inhibitors of SARS-CoV-2 entry: current and future opportunities. J. Med. Chem. 21, 12256–12274.

Yang, Y., Islam, M.S., Wang, J., Li, Y., Chen, X., 2020. Traditional Chinese medicine in the treatment of patients infected with 2019-new coronavirus (SARS-CoV-2): a review and perspective. Int. J. Biol. Sci. 10, 1708–1717.

Yi, T., Leung, K., Lu, G., Zhang, H., Chan, K., 2007. Identification and determination of the major constituents in traditional Chinese medicinal plant *Polygonum multiflorum* Thunb by HPLC coupled with PAD and ESI/MS. Phytochem. Anal. 18, 181–187.